Available online at www.sciencedirect.com
SCIENCE DIRECT®
Journal of Power Sources 130 (2004) 275–280
JOURNAL OF POWER SOURCES
www.elsevier.com/locate/jpowsour

Si–SiC nanocomposite anodes synthesized using high-energy mechanical milling

Il-seok Kim [a], G.E. Blomgren [a,b], P.N. Kumta [a,*]

[a] *Department of Materials Science and Engineering, Carnegie Mellon University, Pittsburgh, PA 15213, USA*
[b] *Blomgren Consulting Services Ltd., 1554 Clarence Avenue, Lakewood, OH 44107, USA*

Received 7 November 2003; accepted 3 December 2003

Abstract

The Si–SiC nanocomposites were synthesized by high-energy mechanical milling (HEMM) using two different starting mixtures, Si:SiC = 1:2 and Si:C = 3:2. Both mixtures result in amorphous silicon and nanocrystalline silicon carbide as confirmed by XRD results. The Si–SiC nanocomposite corresponding to Si:SiC = 1:2 obtained after milling for 30 h shows a capacity as high as ~370 mAh/g. The nanocomposite synthesized using HEMM for 24 h from a mixture corresponding to Si:C = 3:2 also exhibits a stable capacity of ~370 mAh/g. Transmission electron microscopy (TEM) analysis shows that SiC nanocrystallites ≅10 nm in size are distributed homogeneously within the nanocomposite. Electron energy-loss spectroscopy (EELS) maps of C suggests that SiC is uniformly present within the particles.

Keywords: Nanocomposite anodes; HEMM; Amorphous silicon; Silicon carbide

1. Introduction

The need for high-energy density anode materials has led to considerable research to identify alternative materials to carbon, the currently used anode material. In this regard, several researchers have shown the potential of Si or Sn-based systems as alternative anodes, which have very high theoretical capacities compared to the currently used carbonaceous systems [1]. Most of these recent developments to date include generation of nanocomposites of intermetallics comprising electrochemically 'active–inactive' phases [2–9] since Si or Sn anodes have a fatal weakness related to large volume changes associated with alloying and dealloying of lithium followed by structural disintegration of the electrode during electrochemical cycling. Most of the current studies on alternative anode materials other than carbon have focused on creating a composite microstructure comprising an inactive host matrix containing a finely dispersed active phase. Dahn and co-workers [2,3] have reported Sn–Fe–C based nanocomposite, consisting of active Sn_2Fe and almost inactive $SnFe_3C$ and a similar concept of creating the active–inactive composite upon electrochemical insertion of lithium has been explored in the Cu_6Sn_5, InSb and MnSb systems by Thackeray and co-workers [4–6]. Other active–inactive composite systems such as Ni_3Sn_2+C, Mg_3Ni, etc. have been also studied for their potential use as alternative anodes to carbon [8,9]. Although all these systems demonstrate the utility of the active–inactive nanocomposite concept, there is a considerable need to improve the reversible capacity and cyclability.

Our group has demonstrated the potential of Si–TiN and Si–TiB_2 active–inactive nanocomposites synthesized using high-energy mechanical milling (HEMM) for use as anodes in Li-ion batteries [10–13]. The approach provides better flexible control of the final composition since the initial ratio between active and inactive components, which are thermodynamically stable during HEMM, remain unchanged. As discussed, Si–TiN and Si–TiB_2 systems are promising and therefore TiN and TiB_2 appear to be good inactive matrix materials for the use of active–inactive nanocomposites as lithium ion anodes. In order to improve the capacity of the anodes further, it is necessary to use lightweight inactive components and thus, this study was focused on using SiC as an inactive material. In addition, SiC is a very hard material exhibiting hardness of 2500 kg/mm^2 and is also a known wide band-gap semiconductor with electrical resistivity of 10 to 10^2 ohm cm [14]. Nanocomposites containing Si and SiC were therefore synthesized using HEMM. As starting

* Corresponding author. Tel.: +1-412-268-8739; fax: +1-412-268-7596.
E-mail address: kumta@cmu.edu (P.N. Kumta).

0378-7753/$ – see front matter © 2004 Elsevier B.V. All rights reserved.
doi:10.1016/j.jpowsour.2003.12.014

materials, Si, SiC and C were used in order to compare their efficacy for generating Si and SiC nanocomposites.

In the present study, two approaches were used to generate the Si–SiC nanocomposites. The first approach utilized Si and SiC while the second approach employed Si and C. The formation of SiC by reactive milling of Si and C is generally well known [15,16], and hence finer SiC powder can be expected by the latter method. SiC is unlikely to react with Si during mechanical milling and being lighter than TiN and TiB_2, it can be considered a good candidate material for use as an inactive matrix. In this paper, the electrochemical performance of Si–SiC nanocomposites obtained from the two different approaches will be presented. In addition, microstructural analyses using transmission electron microscopy (TEM) have been conducted to identify the microstructure of the nanocomposites that could be deemed necessary for attaining high capacity.

2. Experimental

The general procedure consists of milling commercially obtained materials using an airtight hardened steel vial and the atmosphere inside the vial is preferred to be inert because all materials used in this experiment are very reactive and can be easily oxidized when converted into the nano-sized state. Therefore, all powders were batched in a vial inside an argon filled glove box (VAC atmosphere, Hawthorne, CA, O_2 and moisture content <10 ppm). Two grams of commercial power mixture was sealed in an air-tight vial in a glove box and was mechanically milled subsequently using a SPEX-8000 high-energy mechanical mill with a charge ratio of 25:1 employing 15 hardened steel balls. Two different starting precursors, however, were used to generate the nanocomposites containing identical compositions. The first approach uses 2 g mixture of silicon (Aldrich, 99.5%, 325 mesh) and silicon carbide (Aldrich, 99%, 400 mesh) in a molar ratio of 1:2, while the other approach utilizes a 2g mixtures of silicon (Aldrich, 99.5%, 325 mesh) and carbon (Aldrich, graphite, 99.9%, 1–2 μm) in a molar ratio of 2:3, selected such that a Si–SiC composite of 1:2 molar ratio is obtained in situ during the HEMM process. Milling of both starting mixtures was conducted in an identical manner employing exact conditions.

In order to evaluate the electrochemical characteristics, electrodes were fabricated using the as-milled powder by mixing 87.1 wt.% of the active powder and 7.3 wt.% acetylene black. A solution containing 5.6 wt.% polyvinylidene fluoride (PVDF) in 1-methyl-2-pyrrolidinone (NMP) was added to the mixture. The as-prepared solution was coated onto a Cu foil (INSULECTRO, electro-deposited, thickness: 175 μm). A hockey puck cell design was used employing lithium foil as an anode and 1 M $LiPF_6$ in EC/DMC (2:1) as the electrolyte. All the batteries tested in this study were cycled in the voltage range from 0.02 to 1.2 V employing a current density of 0.1 mA/cm^2 and a minute rest period between the charge/discharge cycles using a potentiostat (Arbin electrochemical instrument). The phases present in the as-milled powders and the cycled electrode were analyzed using X-ray diffraction (Rigaku, θ/θ diffractometer), while the microstructure was examined using a high-resolution transmission electron microscope (Philips Tecnai F20 FEGTEM), equipped with an electron energy-loss spectroscopy (EELS) system and a Gatan energy-loss filter, which allows mapping of the elements within the particles.

3. Results and discussion

Si–SiC nanocomposites were prepared using two different mixtures as mentioned earlier. The first mixture for HEMM comprises commercial Si and SiC. XRD analysis conducted on the nanocomposite containing 33.3 mol% Si obtained after milling Si and SiC for 24 h is shown in Fig. 1(a). The milled powder consists of amorphous-nanocrystalline Si and nanocrystalline β-SiC powder similar to the Si–TiN and Si–TiB_2 nanocomposite systems [10–13]. The XRD pattern

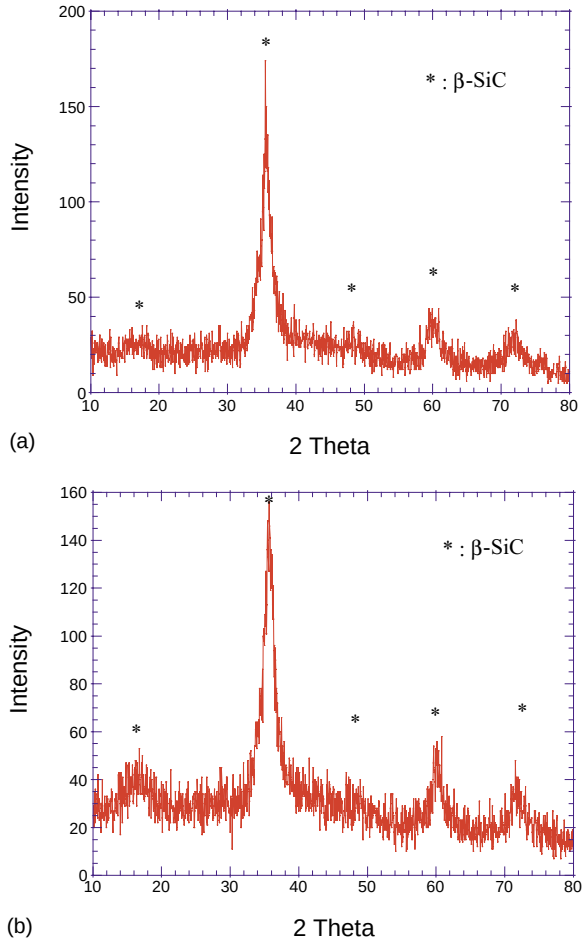

Fig. 1. X-ray diffraction patterns of powders milled for 24 h using HEMM (a) Si:SiC = 1:2, (b) Si:C = 3:2.

collected on the nanocomposite containing 33.3 mol% Si obtained after milling Si and SiC for 12 h, which is not presented, exhibits a very similar pattern to Fig. 1(a), comprising amorphous Si and nanocrystalline β-SiC. The particle sizes of Si and SiC are likely to be different due to the milling action though not significant to be noticeably observed by X-ray diffraction. Milling the mixture of Si and SiC for 30 h also yields a similar XRD pattern although it is very likely that the particle sizes are different. It should be noted that the brittle nature of Si results in rapid pulverization in the presence of the much harder SiC. As a result, the polycrystalline Si is easily converted to its amorphous form. Milling Si alone does not yield amorphous Si even after extended milling for more than 30 h.

The second mixture for generating the Si–SiC nanocomposites is composed of commercial Si and C powders, the composition of which is selected such that the nanocomposite composition after milling is identical to the first mixture. Since Si and C react to form an incongruently melting stoichiometric compound of SiC (Si:C = 50:50) based on the phase diagram of Si–C [17], the composition of the mixture corresponding to the molar ratio of Si:C = 3:2 will generate the Si–SiC nanocomposite containing 33.3 mol% of Si after the mechanochemical synthesis of SiC. It has also been reported that Si and C with an identical molar ratio can generate stoichiometric SiC without any unreacted Si or C [17]. The XRD spectra obtained on the powder which is synthesized using a mixture of Si and C after milling for 24 h (Fig. 1(b)), shows an almost identical pattern with (a), comprising amorphous Si and nanocrystalline β-SiC phases. This result confirms that the mechanochemical reaction between Si and C occurs at the early stages of milling and the SiC formed during milling helps to pulverize the Si powder.

Fig. 2(a) shows the specific capacity vs. cycle number for the Si–SiC nanocomposites synthesized using Si and SiC. All the milled samples correspond to a molar ratio 1:2. The advantages of using SiC as the matrix component is first to prevent any possible reaction between Si and the matrix since the only possible compound in the Si–C system is stoichiometric SiC based on the Si–C phase diagram and second, to reduce the weight of the inactive matrix component. As a consequence, capacity retention is enhanced even after extended milling while maintaining the desired capacity. However, as seen from the plot, the capacity decreases with increase in milling time suggesting other possible reasons contributing to the decrease in capacity such as embedding of the active Si phase. Experimental studies identifying the exact cause of this reduction in capacity after mechanical milling will be published subsequently. Although there is a small fade in capacity (∼1.7% loss per cycle), the samples milled for 30 h show a capacity as high as ∼370 mAh/g after 15 cycles using a constant current of 100 μA/cm^2 corresponding to a C-rate of ∼C/25.

As discussed in the Si–TiB_2 nanocomposites prepared using premilled TiB_2 powders [13], the fine initial particle size of the inactive matrix before milling improves the electrochemical stability of the anode capacity. It was therefore decided to explore the use of Si and C as starting materials for milling instead of Si and SiC, since SiC generated during the milling process is expected to be much finer. The anode synthesized using Si and C mixture is tested and its electrochemical characteristics are shown in Fig. 2(b). The molar ratio of the initial composition used for milling corresponds to Si:C = 3:2, which ultimately yields an overall molar ratio of Si–SiC of 1:2 assuming complete consumption of C with Si to form SiC. Although it is difficult to unequivocally distinguish the two different samples made by the different experimental approaches, it appears that Si–SiC nanocomposites prepared using Si and C mixture show better capacity retention (∼0.9% loss per cycle) due to the fine particle size of the inactive component although they exhibit similar capacity values of ∼370 mAh/g after 15 cycles using a constant current of 100 μA/cm^2 corresponding to a C-rate of ∼C/25.

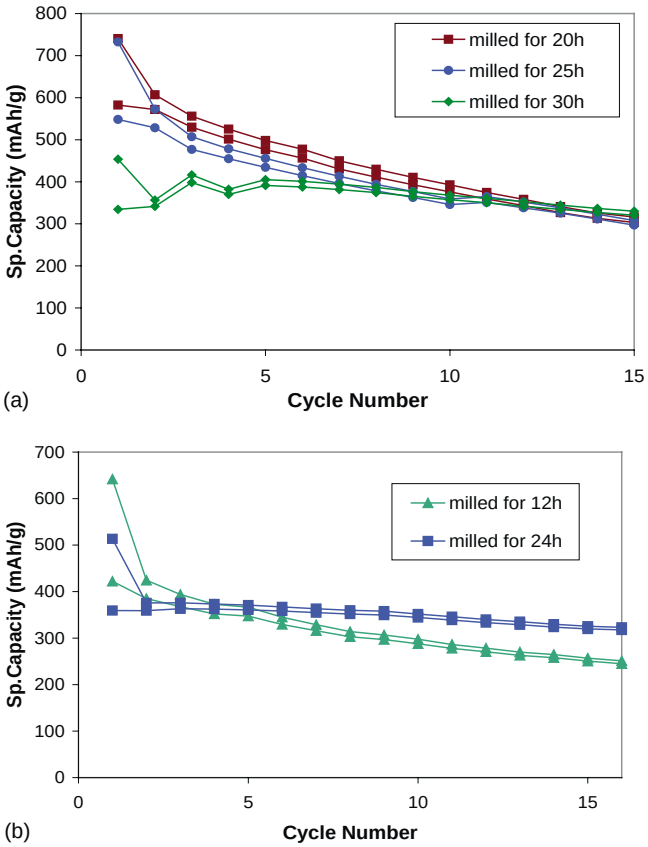

Fig. 2. Capacity as a function of cycle number for Si–SiC nanocomposites obtained after milling for different time periods. (a) Si and SiC using the molar ratio of Si:SiC = 1:2, (b) Si and C using the molar ratio of Si:C = 3:2. Current rate: 100 μA/cm^2, potential: 0.02–1.2 V.

The differential capacity of the nanocomposite samples prepared from Si:SiC = 1:2 obtained after milling for 30 h and from a Si:C = 3:2 sample obtained after milling for 24 h, are shown in Fig. 3(a) and (b), respectively. Both plots corresponding to the electrodes appear to be almost identical, suggesting that the two samples are very similar

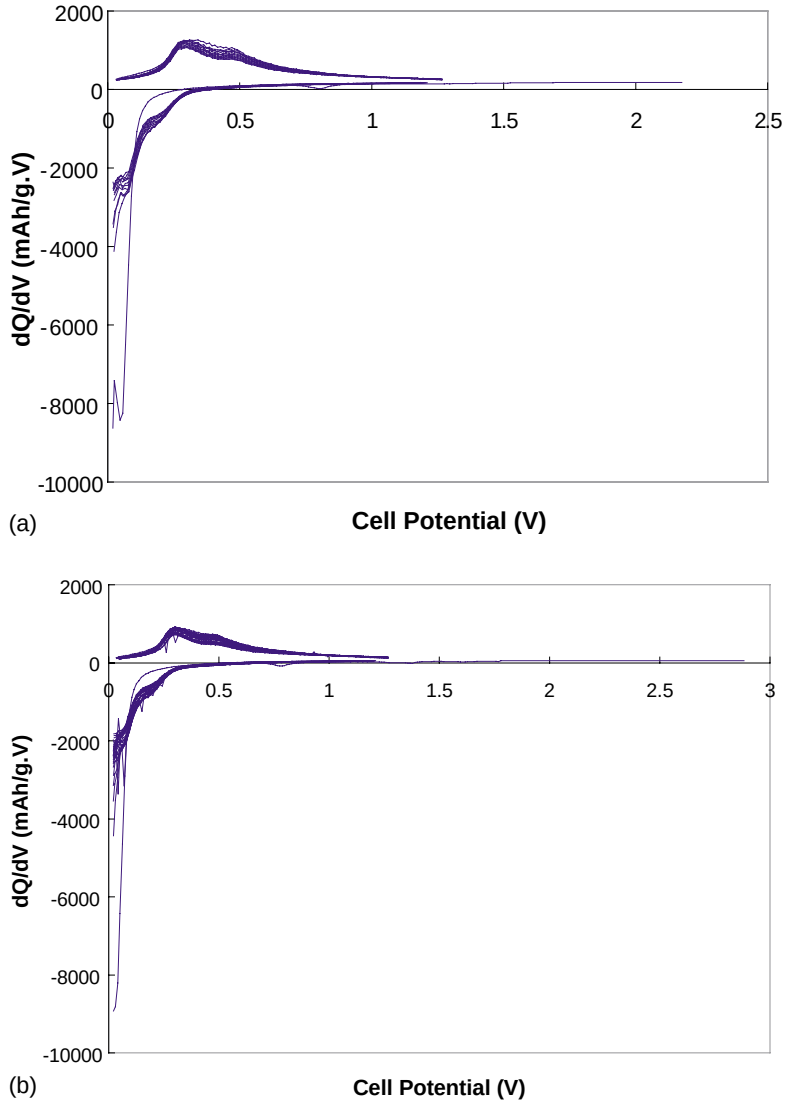

Fig. 3. The differential capacity plots of the nanocomposites prepared from (a) Si:SiC = 1:2 obtained after milling for 30 h and (b) Si:C = 3:2 obtained after milling for 24 h. Current rate: 100 μA/cm^2, potential: 0.02–1.2 V.

from the viewpoint of electrochemical behavior. The two broad peaks during charge and discharge cycles (≅0.08, 0.2; ≅0.3, and 0.45 V) are attributed to the reaction of amorphous Si with Li. Although both nanocomposites exhibit very similar differential capacity behavior related to the reaction of nanosized Si particles in the nanocomposites, the Si–SiC nanocomposite obtained from Si:C = 3:2 mixture exhibits better capacity retention than the one obtained from Si:SiC = 1:2 mixture. This is mainly due to the finer size of the inactive component, which is generated in situ during the HEMM process, although the electrochemical response from the differential capacity appears to be similar. Microstructural study was therefore conducted on the Si–SiC nanocomposite obtained after milling Si:C = 3:2 mixture for 24 h.

In order to investigate the microstructure of the Si–SiC nanocomposite obtained from Si and C, high-resolution transmission electron microscopy (HRTEM) was conducted on the nanocomposite of Si:C = 3:2 ratio obtained after milling for 24 h and the resulting micrographs are shown in Figs. 5(a) and (b). The bright field image and dark field image indicate the presence of very fine size SiC crystallites (10–20 nm) seen as dark and white regions in the BF and DF images, respectively within the agglomerates (≅100 nm) (see Fig. 4(a) and (b)), which is similar to the other nanocomposites obtained after HEMM discussed in the previous work [12,13]. The selected area diffraction pattern (SADP) exhibits well-defined rings with some spots which have been indexed to β-SiC (see Fig. 4(d)), suggesting the nanocrystalline nature of the β-SiC nanosized particles. No presence of crystalline Si is seen in the SADP validating the amorphous nature of Si as indicated by XRD. The image in Fig. 4(c) shows the agglomeration of Si–SiC nanocomposite particles, although the dark regions corresponding to SiC nanocrystallites are not shown clearly in comparison to the BF image (Fig. 4(a)) due to the lower

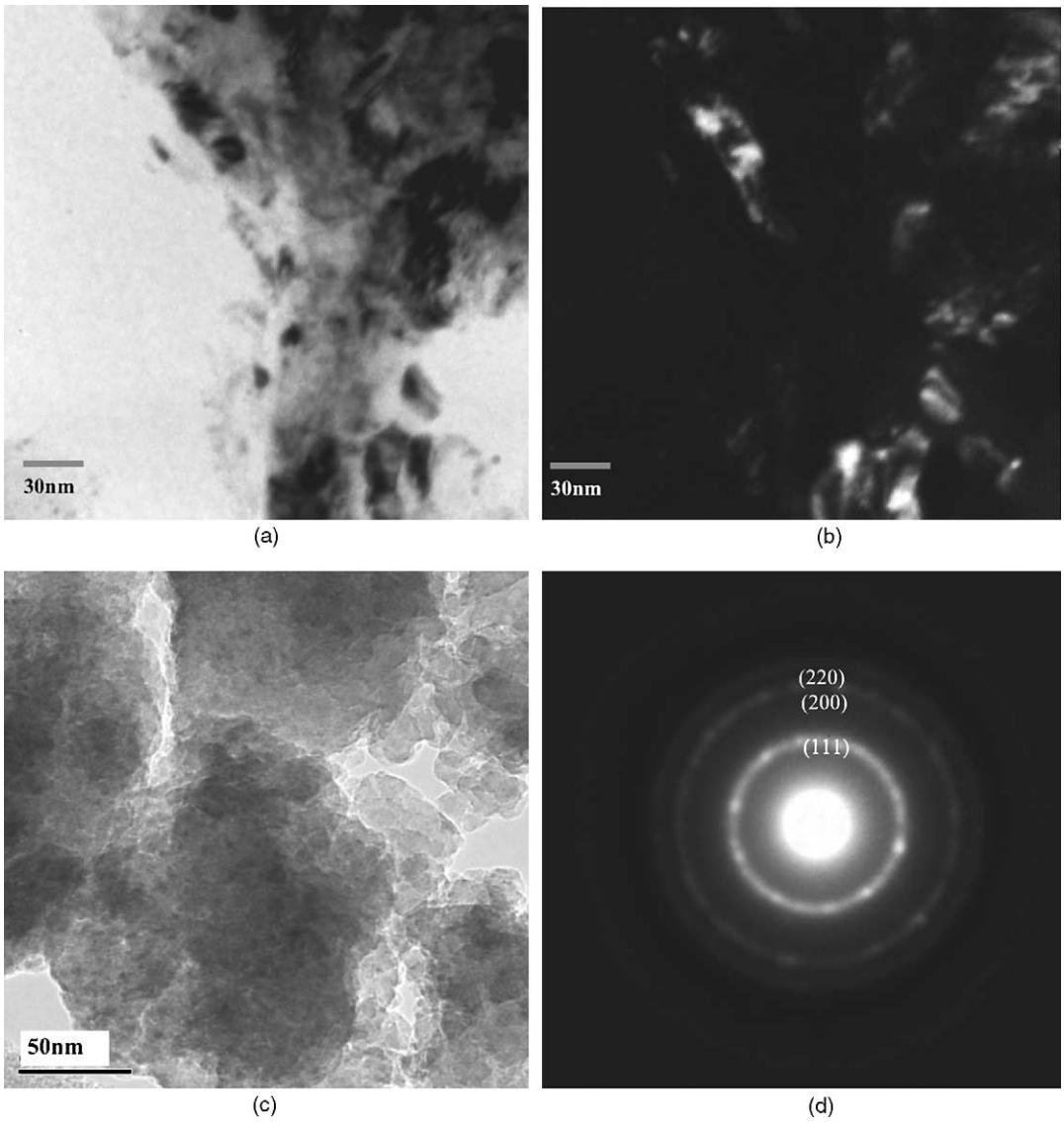

Fig. 4. TEM micrographs of the Si–SiC nanocomposite obtained after milling Si and C in the molar ratio (Si:C = 3:2) for 24 h. (a) BF image, (b) DF image, (c) BF image at a lower magnification, and (d) SA diffraction pattern (camera length=66 cm, reduced to 70% of its original size).

magnification. The nanocomposite has been examined at high magnifications due to the fine particle size and severe agglomeration of the particles. At the same time, the distribution of carbon has been studied using EELS to map the presence of SiC and Si in the nanocomposite.

Fig. 5(a) shows the high-resolution image of the nanocomposite corresponding to Si:SiC = 1:2 obtained after milling Si and C in the molar ratio of Si:C = 3:2 for 24 h The marked areas showing the lattice fringes correspond to the nanocrystalline β-SiC that has a particle size of 5–10 nm. The surrounding areas correspond to amorphous Si and not as clearly visible in the BF image. Hence, an elemental map of carbon has been obtained using electron energy-loss spectroscopy, the results of which are shown in Fig. 5(b). Carbon was selected as the element for mapping in these nanoscale regions since silicon is present in both the active and inactive matrix components. Hence, in the case of Si, a clear map was not achieved. The bright regions correspond to SiC nanocrystallites, which indicate the regions with high concentration of carbon as mentioned earlier in the case of Si–TiN nanocomposites. The elemental map of carbon reveals two distinct regions according to carbon concentration where Si and SiC are homogeneously distributed in the composite at a nanoscale. The microstructure of the nanocomposite appears to be slightly different from that of the Si–TiN nanocomposites. In the case of the Si–TiN, TiN particles are uniformly coated with finely milled amorphous silicon, whereas in the Si–SiC nanocomposites, the β-SiC particles are irregular in shape. This may be possibly caused by the in situ chemical reaction between silicon and carbon that is responsible for generating β-SiC nanocrystallites in contrast to TiN. TiN nanocrystallites are

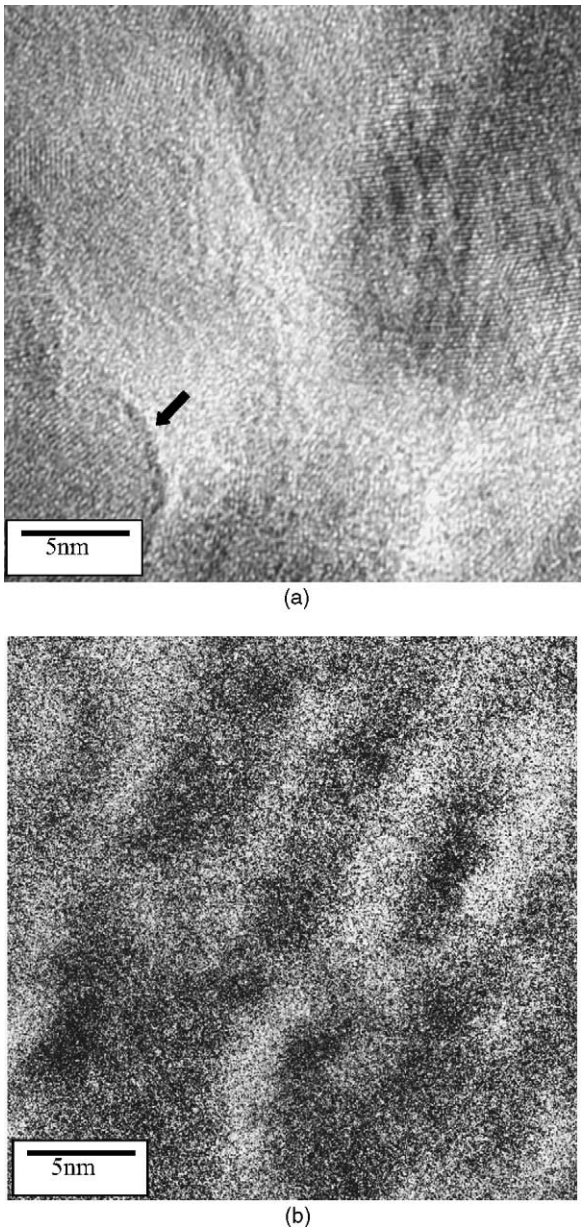

Fig. 5. (a) HRTEM micrograph of the Si–SiC nanocomposite obtained after milling Si and C in the molar ratio (Si:C = 3:2) for 24 h. The marked region shows the lattice fringes corresponding to nanocrystalline SiC. (b) Elemental map of carbon, which is analyzed by electron energy-loss spectroscopy.

generated by pulverization of TiN polycrystals while SiC nanocrystallites are generated from the diffusional chemical reaction between Si and C during HEMM. Hence, β-SiC particles tend to have an irregular shape as shown in Fig. 4. These results nevertheless suggest that the Si–SiC nanocomposites comprise two phases, amorphous Si and nanocrystalline β-SiC analogous to the case of Si–TiN and Si–TiB_2. The study also indicates that the HEMM process is a useful method to generate nanocomposites by reacting Si and carbon to form SiC, an electrochemically inactive component.

4. Conclusion

Two different mixtures comprising Si:SiC = 1:2 and Si:C = 3:2, respectively result in the nanocomposites of amorphous Si and nanocrystalline SiC. Both nanocomposites obtained from the mixtures of Si:SiC = 1:2 and Si:C = 3:2 after milling for 30 and 24 h each exhibit a capacity as high as ∼370 mAh/g, although the nanocomposite obtained from Si:C = 3:2 mixture shows better stability due to fine particle size of inactive matrix component. The result of HRTEM shows that SiC nanocrystallites corresponding to particle size of ≅10 nm are distributed homogeneously within the Si–SiC nanocomposite. EELS mapping of carbon indicates that SiC is uniformly present within the particles.

Acknowledgements

P.N. Kumta, Il-seok Kim and G.E. Blomgren would like to thank the financial support of NSF (Grants CTS-9700343 and CTS-0000563), NASA (NAG3-2640) and ONR (Grant N00014-00-1-0516) for this work.

References

[1] M. Winter, J.O. Besenhard, Electrochim. Acta 45 (1999) 31.
[2] O. Mao, R.L. Turner, I.A. Courtney, B.D. Fredericksen, M.I. Buckett, L.J. Krause, J.R. Dahn, Electrochem. Solid-State Lett. 2 (1999) 3.
[3] O. Mao, J.R. Dahn, J. Electrochem. Soc. 146 (1999) 405.
[4] K.D. Kepler, J.T. Vaughey, M.M. Thackeray, Electrochem. Solid-State Lett. 2 (1999) 307.
[5] J.T. Vaughey, J. O'Hara, M.M. Thackeray, Electrochem. Solid-State Lett. 3 (2000) 13.
[6] L.M.L. Fransson, J.T. Vaughey, K. Edstrom, M.M. Thackeray, J. Electrochem. Soc. 150 (2003) A86.
[7] J. Yang, M. Wachtler, M. Winters, J.O. Besenhard, Electrochem. Solid-State Lett. 2 (1999) 161.
[8] G.M. Ehrlich, C. Durand, X. Chen, T.A. Hugener, F. Spiess, S.L. Suib, J. Electrochem. Soc. 147 (2000) 886.
[9] H. Kim, B. Park, H. Sohn, T. Kang, J. Power Sources 90 (2000) 59.
[10] I.S. Kim, G.E. Blomgren, P.N. Kumta, Electrochem. Solid-State Lett. 3 (2000) 493.
[11] I.S. Kim, G.E. Blomgren, P.N. Kumta, Ceram. Trans. 249 (2002) 35.
[12] I.S. Kim, G.E. Blomgren, P.N. Kumta, Ceram. Trans. 249 (2002) 127.
[13] I.S. Kim, G.E. Blomgren, P.N. Kumta, Electrochem. Solid-State Lett. 6 (2003) A157.
[14] F. Cardalrelli, Material Handbook A Concise Desktop Reference, Springer, London, 2000.
[15] R. Ren, Z. Yang, L.L. Shaw, J. Am. Ceram. Soc. 85 (2002) 819.
[16] L.L. Shaw, Z. Yang, R. Ren, J. Am. Ceram. Soc. 85 (2002) 709.
[17] M.S.E. Eskandarany, K. Sumiyama, K. Suzuki, J. Mater. Res. 10 (1995) 659.